Proceedings of the 28th IEEE
EMBS Annual International Conference
New York City, USA, Aug 30-Sept 3, 2006

Computing the 3-D structure of viruses from unoriented cryo electron microscope images: a fast algorithm for a statistical approach

Junghoon Lee, Yili Zheng, and Peter C. Doerschuk

Abstract— **In a cryo electron microscopy experiment, the data is noisy 2-D projection images of the 3-D electron scattering intensity where the orientation of the projections is not known. In previous work we have developed a solution for this problem based on a maximum likelihood estimator that is computed by an expectation maximization algorithm. In the expectation maximization algorithm the expensive step is the expectation which requires numerical evaluation of 3- or 5-dimensional integrations of a square matrix of dimension equal to the number of Fourier series coefficients used to describe the 3-D reconstruction. By taking advantage of the rotational properties of spherical harmonics, we can reduce the integrations of a matrix to integrations of a scalar. The key property is that a rotated spherical harmonic can be expressed as a linear combination of the other harmonics of the same order and the weights in the linear combination factor so that each of the three factors is a function of only one of the Euler angles describing the orientation of the projection. Numerical example of the reconstructions is provided based on Nudaurelia Omega Capensis Virus.**

I. INTRODUCTION

Cryo electron microscopy (cryo EM) is an important method for determining the 3-D structure of macromolecular molecules and viruses. In this method, the electron microscopy fundamentally provides the 2-D projection of the 3-D electron scattering intensity of the particle. Because the particles are rapidly damaged by the electron beam, the beam current is minimized and only one projection from each of a large collection of identical particles are measured. Because the particles are unoriented in the microscope, using one projection of each of a large number of identical particles implies that the projection directions are not known. This makes the inverse problem fundamentally nonlinear. Minimization of the beam current implies that the images are noisy, with signal to noise ratio (SNR) well below 1. The poor SNR implies that the location of the center of the projected image is uncertain. Finally, the images are not actually projections because the optics of the microscope contribute a so-called contrast transfer function which is a linear system dependent only on the magnitude of the 2-D image spatial frequency vector and which has zeros and zero crossings in the spatial frequency range of interest. We describe the noise in the image as additive white Gaussian noise with zero mean and constant variance. Based on the projection slice theorem, the resulting equation describing the 2-D Fourier transform of the noisy image is

$$\Sigma(\boldsymbol{\kappa}) = \exp(-i2\pi\boldsymbol{\kappa}\cdot\boldsymbol{\chi}_0)G(\kappa)P(R^{-1}_{\alpha\beta\gamma}(\boldsymbol{\kappa}^T,0)^T) + N(\boldsymbol{\kappa}) \quad (1)$$

where $\boldsymbol{\kappa} \in \mathbb{R}^2$ is the spatial frequency vector in the image Fourier transform, $\boldsymbol{\chi}_0 \in \mathbb{R}^2$ is the unknown center of the projected image, $G(\cdot)$ is the contrast transfer function, $P(\cdot)$ is the 3-D Fourier transform of the electron scattering intensity, $R_{\alpha\beta\gamma} \in \mathbb{R}^{3\times3}$ is the rotation matrix (parameterized by Euler angles (α,β,γ)) that describes the projection direction, and $N(\cdot)$ is the 2-D Fourier transform of the pixel noise which is therefore also white Gaussian noise with zero mean and constant variance.

In many biological experiments, the specimen contains a mixture of more than one type of virus or more than one state of a single type of virus. Because the SNR is low and the image only shows roughly projection information rather than 3-D information, classification of each virus image into the correct class is challenging. One approach to this problem is to combine classification and reconstruction by estimating multiple reconstructions simultaneously from data that has an unmeasured label describing the virus class from which it originates. When the label has a known probability mass function, which is the case we have considered, either maximization of the marginal log likelihood function which results from integrating out the label by direct nonlinear programming or by an expectation maximization algorithm where the hidden data includes the label, can be performed [1], [2], [3]. This approach is successful and several examples for two-class cases are demonstrated in [4], [5].

While this algorithm is successful and enjoys all the statistical advantages of a maximum likelihood estimator, it is costly to compute. The computational cost has motivated a search for alternative representations of the same estimator which have faster implementations and one such representation is described in the remainder of this paper.

II. THE FAST ALGORITHM

A. An invertible linear transformation of the data

Because the noise model is additive white Gaussian pixel noise, any linear transformation of the images leads to a new estimation problem which also has an additive Gaussian pixel noise model. If the transformation is essentially Fourier in nature, then the white property of the noise in the original

This work was supported by NSF Grants CCR-0098156, EIA-0112672, and CCR-0325544 and NIH Grant 1R01EB000432-01.

J. Lee is with the School of Electrical and Computer Engineering, Purdue University, West Lafayette, IN 47907, USA junghoon@purdue.edu.

Y. Zheng is with the School of Electrical and Computer Engineering, Purdue University, West Lafayette, IN 47907, USA yzheng@ecn.purdue.edu.

P. C. Doerschuk is a Professor of the School of Electrical and Computer Engineering, Purdue University, West Lafayette, IN 47907, USA doerschu@ecn.purdue.edu. Corresponding author.

problem is also preserved by the transformation. If the transformation is invertible, then the two problems imply equivalent estimators. Described in polar coordinates, the 2-D Fourier transform of the image is periodic in the angular variable and therefore can be expanded in a Fourier series in the angular variable with radially-dependent weights, e.g., [6]. The starting point of the fast algorithm is to take the images, apply this transformation, and then solve the resulting Gaussian estimation problem. The interesting fact is that the log likelihood for the resulting estimation problem can be computed with less effort than for the original problem.

For $\boldsymbol{\chi}, \boldsymbol{\kappa} \in \mathbb{R}^2$ let $\sigma(\boldsymbol{\chi})$ be an image and $\Sigma(\boldsymbol{\kappa})$ be its 2-D Fourier transform:

$$\Sigma(\boldsymbol{\kappa}) \doteq \int \sigma(\boldsymbol{\chi}) \exp(-i2\pi\boldsymbol{\chi}\cdot\boldsymbol{\kappa})\mathrm{d}^2\boldsymbol{\chi}.$$

It can be shown that

$$\Sigma(\boldsymbol{\kappa}) = \sum_{m=-\infty}^{+\infty} \Sigma_m(\kappa) e^{im\psi'}$$

where $\Sigma_m(\kappa)$ has two important forms:

$$\begin{aligned}\Sigma_m(\kappa) &= \frac{1}{2\pi}\int_0^{2\pi} \Sigma(\boldsymbol{\kappa})\exp(-im\psi')\mathrm{d}\psi' \\ &= (-i)^{|m|}\int\int \sigma(\chi,\psi)\exp(-im\psi)J_{|m|}(2\pi\kappa\chi)\chi\mathrm{d}\chi\mathrm{d}\psi.\end{aligned}$$

B. The mathematical model for the scattering intensity

Describe the electron scattering intensity $\rho(\mathbf{x})$ by an orthonormal harmonic series in spherical coordinates:

$$\rho(\mathbf{x}) = \sum_{l=0}^{\infty}\sum_{m=-l}^{+l}\sum_{p=1}^{\infty} c_{l,m,p} h_{l,p}(x)\Psi_{l,m}(\theta,\phi).$$

Then $P(\mathbf{k})$, the 3-D Fourier transform of $\rho(\mathbf{x})$ can be computed analytically with the result that

$$P(\mathbf{k}) = \sum_{l=0}^{\infty}\sum_{m=-l}^{+l}\sum_{p=1}^{\infty} c_{l,m,p}(-i)^l H_{l,p}(k)\Psi_{l,m}(\theta',\phi').$$

C. Rotations and projections

Define ρ' in terms of ρ by $\rho'(\mathbf{x}) = \rho(R^{-1}_{\alpha\beta\gamma}\mathbf{x})$ and compute its 3-D Fourier transform to get that

$$\begin{aligned}P'(\mathbf{k}) &= \sum_{m=-\infty}^{+\infty}\sum_{l=|m|}^{\infty}\sum_{m'=-l}^{+l}\sum_{p=1}^{\infty} c_{l,m,p}(-i)^l H_{l,p}(k) \\ &\quad\times \left[\sum_{m''=-l}^{+l} b_{l,m',m''} D^l_{m,m''}(\alpha,\beta,\gamma)\right] \\ &\quad\times Y_{l,m}(\theta',0)e^{im\phi'} \qquad (2)\end{aligned}$$

where $D^l_{m,m''}(\alpha,\beta,\gamma)$ are the Wigner coefficients [7] and the original harmonics $\Psi_{l,m}(\theta,\phi)$ are expressed in terms of spherical harmonics [8, Eq. 3.53] by

$$\Psi_{l,m}(\theta,\phi) \doteq \sum_{m'=-l}^{+l} b_{l,m,m'} Y_{l,m'}(\theta,\phi).$$

Equation (2) is a Fourier series in the ϕ' variable (fundamental period of 2π).

Let ω be the z-directed projection of ρ' and relate the 2-D Fourier transform of ω (denoted by Ω) to the 3-D Fourier transform of ρ':

$$\begin{aligned}\omega(\boldsymbol{\chi}) &= \int \rho'((\boldsymbol{\chi}^T, z)^T)\mathrm{d}z \\ \Omega(\boldsymbol{\kappa}) &= \sum_{m=-\infty}^{+\infty}\Omega_m(\kappa)e^{im\psi'} \\ \Omega_m(\kappa) &= e^{-im\alpha}\sum_{l=|m|}^{\infty}\sum_{m'=-l}^{+l}\sum_{p=1}^{\infty}(-i)^l H_{l,p}(\kappa)Y_{l,m}(\frac{\pi}{2},0) \\ &\quad\times \left[\sum_{m''=-l}^{+l} b_{l,m',m''} d^l_{m,m''}(\beta)e^{-im''\gamma}\right] c_{l,m',p}. \qquad (3)\end{aligned}$$

D. The linear transformation of the imaging equation

Denote the measurements $y(\boldsymbol{\chi})$ and its 2-D Fourier tansform $Y(\boldsymbol{\kappa})$ (previously denoted by $\sigma(\boldsymbol{\chi})$ and $\Sigma(\boldsymbol{\kappa})$, respectively) and multiply both sides of (1) by $\exp(i2\pi\boldsymbol{\kappa}^T\boldsymbol{\chi}_0)$ to get

$$\begin{aligned}Y(\boldsymbol{\kappa})\exp(i2\pi\boldsymbol{\kappa}\cdot\boldsymbol{\chi}_0) &= G(\kappa)\Omega(\boldsymbol{\kappa}) + N'(\boldsymbol{\kappa}) \\ N'(\boldsymbol{\kappa}) &\doteq N(\boldsymbol{\kappa})\exp(i2\pi\boldsymbol{\kappa}\cdot\boldsymbol{\chi}_0).\end{aligned}$$

Since N' is the Fourier transform of $n'(\boldsymbol{\chi}) = n(\boldsymbol{\chi}+\boldsymbol{\chi}_0)$ and n is WSS it follows that the statistical properties of N' are the same as the statistical properties of N. Define notations for the mth ψ' Fourier series coefficients of both sides by

$$\begin{aligned}Y'_m(\kappa) &\doteq \frac{1}{2\pi}\int Y(\boldsymbol{\kappa})\exp(i2\pi\boldsymbol{\kappa}\cdot\boldsymbol{\chi}_0)\exp(-im\psi')\mathrm{d}\psi' \\ L_m(\kappa) &\doteq G(\kappa)\frac{1}{2\pi}\int\Omega(\boldsymbol{\kappa})\exp(-im\psi')\mathrm{d}\psi' \\ &= G(\kappa)\Omega_m(\kappa) \qquad (4) \\ N'_m(\kappa) &\doteq \frac{1}{2\pi}\int N'(\boldsymbol{\kappa})\exp(-im\psi')\mathrm{d}\psi'\end{aligned}$$

and equate the coefficients to get the result that

$$Y'_m(\kappa) = L_m(\kappa) + N'_m(\kappa) \qquad (5)$$

for $m \in \mathcal{Z}$ and $\kappa \in [0,\infty)$.

Using the previous types of calculation, we can express $Y'_m(\kappa)$ in terms of $Y(\boldsymbol{\kappa})$ or $Y_m(\kappa)$:

$$\begin{aligned}&Y'_m(\kappa) \\ &\doteq \frac{1}{2\pi}\int Y(\boldsymbol{\kappa})\exp(i2\pi\boldsymbol{\kappa}\cdot\boldsymbol{\chi}_0)\exp(-im\psi')\mathrm{d}\psi' \qquad (6) \\ &= \sum_{m'=-\infty}^{+\infty} Y_{m-m'}(\kappa)i^{|m'|}e^{-im'\psi_0}J_{|m'|}(2\pi\kappa\chi_0) \qquad (7) \\ &= \sum_{m'=-\infty}^{+\infty} Y_{m'}(\kappa)i^{|m-m'|}e^{-i(m-m')\psi_0} \\ &\quad\times J_{|m-m'|}(2\pi\kappa\chi_0). \qquad (8)\end{aligned}$$

Using one of (6), (7), or (8), it is possible to compute $Y'_m(\kappa)$ from the Fourier transforms of the original images as a

function of $\boldsymbol{\chi}_0$. Alternatively, $Y'_m(\kappa)$ can be computed from the $\boldsymbol{\chi}_0$ translates of the original images since

$$y'(\boldsymbol{\chi}) \quad = \quad y(\boldsymbol{\chi}+\boldsymbol{\chi}_0).$$

The statistics of the $N'_m(\kappa)$ term can be determined by direct computation. Assume that

$$\begin{aligned} R_{n',n'}(\boldsymbol{\chi}_1,\boldsymbol{\chi}_2) &= R_{n,n}(\boldsymbol{\chi}_1+\boldsymbol{\chi}_0,\boldsymbol{\chi}_2+\boldsymbol{\chi}_0) \\ &= \frac{N_0}{2}\delta(\boldsymbol{\chi}_1-\boldsymbol{\chi}_2). \end{aligned}$$

Then, $E[N'_m(\kappa)] = 0 + i0$, and

$$\begin{aligned} &E[\Re N'_{m_1}(\kappa_1)\Re N'_{m_2}(\kappa_2)] \\ &\quad = \frac{1}{2}\frac{N_0}{2}\delta(\kappa_1-\kappa_2)\left[\delta_{m_1,m_2}+\delta_{m_1,-m_2}(-1)^{|m_1|}\right] \\ &E[\Im N'_{m_1}(\kappa_1)\Im N'_{m_2}(\kappa_2)] \\ &\quad = \frac{1}{2}\frac{N_0}{2}\delta(\kappa_1-\kappa_2)\left[\delta_{m_1,m_2}-\delta_{m_1,-m_2}(-1)^{|m_1|}\right] \\ &E[\Re N'_{m_1}(\kappa_1)\Im N'_{m_2}(\kappa_2)] = E[\Im N'_{m_1}(\kappa_1)\Re N'_{m_2}(\kappa_2)] = 0. \end{aligned}$$

E. Expressions in terms of matrices

The previous results can be written in matrix form as follows. Combine (3) and (4) to get

$$\begin{aligned} L_m(\kappa) &= G(\kappa)e^{-im\alpha}\sum_{l=|m|}^{\infty}\sum_{m'=-l}^{+l}\sum_{p=1}^{\infty}(-i)^l H_{l,p}(\kappa) \\ &\times \left[\sum_{m''=-l}^{+l} b_{l,m',m''}d^l_{m,m''}(\beta)e^{-im''\gamma}\right] \\ &\times Y_{l,m}(\pi/2,0)c_{l,m',p}. \end{aligned} \tag{9}$$

Define the matrix implied by (9): Define $L \in \mathbb{R}^{\infty\times\infty}$ with elements $L_{m,\kappa;l,m',p}$ where the rows are indexed by the pair m,κ and the columns are indexed by the triple l,m',p and where

$$\begin{aligned} L_{m,\kappa;l,m',p} &\doteq G(\kappa)e^{-im\alpha}(-i)^l H_{l,p}(\kappa) \\ &\times \left[\sum_{m''=-l}^{+l} b_{l,m',m''}d^l_{m,m''}(\beta)e^{-im''\gamma}\right] \\ &\times Y_{l,m}(\pi/2,0). \end{aligned} \tag{10}$$

Define $c \in \mathbb{R}^{\infty}$ with components $c_{l,m',p}$ indexed by the triple l,m',p. Define $Y' \in \mathbb{R}^{\infty}$ with components $Y'_m(\kappa)$ indexed by the pair m,κ. Define $N' \in \mathbb{R}^{\infty}$ with components $N'_m(\kappa)$ indexed by the pair m,κ. Then, (5) is equivalent to

$$Y' \quad = \quad Lc + N'. \tag{11}$$

There are two steps to reducing this to a finite set of equations. First, the range of the m, l, m', and p indices must be truncated to finite values as in [1]. Second, the κ index must be sampled. From both a physical point of view and from a statistical point of view, the natural representation of sampling is to average over small regions in κ. The definition of the averaged noise is

$$w_{m,j} \quad \doteq \quad \frac{2}{\kappa^2_{j+1}-\kappa^2_j}\int_{\kappa_j}^{\kappa_{j+1}} N'_m(\kappa)\kappa\mathrm{d}\kappa$$

where the integration measure is $\kappa\mathrm{d}\kappa$ rather than $\mathrm{d}\kappa$ because it is natural to average in a ring (inner radius κ_j, outer radius κ_{j+1}) when computing $N'_m(\kappa)$ from $N'(\boldsymbol{\kappa})$ and the normalizer is

$$\int_{\kappa_j}^{\kappa_{j+1}} \kappa\mathrm{d}\kappa \quad = \quad \frac{1}{2}\left(\kappa^2_{j+1}-\kappa^2_j\right).$$

The noise $w_{m,j}$ is clearly white in both indices, since $N'_m(\kappa)$ is white in both m and κ. The second order statistics are

$$\begin{aligned} &E[\Re w_{m_1,j_1}\Re w_{m_2,j_2}] \\ &= \delta_{j_1,j_2}\left[\delta_{m_1,m_2}+\delta_{m_1,-m_2}(-1)^{|m_1|}\right]\frac{2}{3}\frac{\kappa^3_{j_1+1}-\kappa^3_{j_1}}{(\kappa^2_{j_1+1}-\kappa^2_{j_1})^2}\frac{N_0}{2} \\ &E[\Im w_{m_1,j_1}\Im w_{m_2,j_2}] \\ &= \delta_{j_1,j_2}\left[\delta_{m_1,m_2}-\delta_{m_1,-m_2}(-1)^{|m_1|}\right]\frac{2}{3}\frac{\kappa^3_{j_1+1}-\kappa^3_{j_1}}{(\kappa^2_{j_1+1}-\kappa^2_{j_1})^2}\frac{N_0}{2} \\ &E[\Re w_{m_1,j_1}\Im w_{m_2,j_2}] = E[\Im w_{m_1,j_1}\Re w_{m_2,j_2}] = 0. \end{aligned}$$

F. Origin of the "fast" character of the algorithm

The fast character of the algorithm is due to the factor $e^{-im\alpha}$ in (10). Conditional on the values of the origin location $\boldsymbol{\chi}_0$ and the Euler angles (α,β,γ), (11) describes a linear Gaussian estimation problem with likelihood function

$$p(Y'|c,\boldsymbol{\chi}_0,(\alpha,\beta,\gamma)) \quad = \quad N(L(\boldsymbol{\chi}_0,(\alpha,\beta,\gamma))c,Q)(Y')$$

where the dependence of L on $\boldsymbol{\chi}_0$ and (α,β,γ) has been made explicit and Q is the covariance matrix. The marginal likelihood function is

$$\begin{aligned} p(Y'|c) &= \int N(L(\boldsymbol{\chi}_0,(\alpha,\beta,\gamma))c,Q)(Y') \\ &\times p(\boldsymbol{\chi}_0)p(\alpha,\beta,\gamma)\mathrm{d}^2\boldsymbol{\chi}_0\mathrm{d}(\alpha,\beta,\gamma) \end{aligned} \tag{12}$$

where $p(\boldsymbol{\chi}_0)$ is the probability density function (pdf) on $\boldsymbol{\chi}_0$, $p(\alpha,\beta,\gamma)$ is the pdf on (α,β,γ), and $\mathrm{d}(\alpha,\beta,\gamma)$ indicates integration over Haar measure for the group of rotations (i.e., special orthogonal matrices in $R^{3\times3}$). The integral indicated in (12) cannot be done analytically and, in fact, represents the bulk of the numerical computation. From the exponent of the Gaussian the integral contains terms L^HL. Because the only dependence of L on α is due to the factor $e^{-im\alpha}$ in (10), terms L^HL can be moved outside of the α integration. As described in [1], [3], the solution of the maximum likelihood estimation problem requires integrating an integrand that contains a factor of L^HL. The dimension of this matrix is equal to the number of unknown $c_{l,m,p}$ coefficients, which is $\gg 10^2$. Therefore, the ability to move the L^HL term outside of the α integration is a major improvement in computational cost and this change is the fast algorithm.

III. NUMERICAL RESULTS

In this section, we describe the numerical results concerning both reconstruction and the speed of the previous and the fast algorithms. We compute the 3-D structure of the capsid of Nudaurelia Omega Capensis Virus (*NωV*) [9] from synthetic images based on the atomic resolution structure of the capsid of *NωV*. Because the true structure from

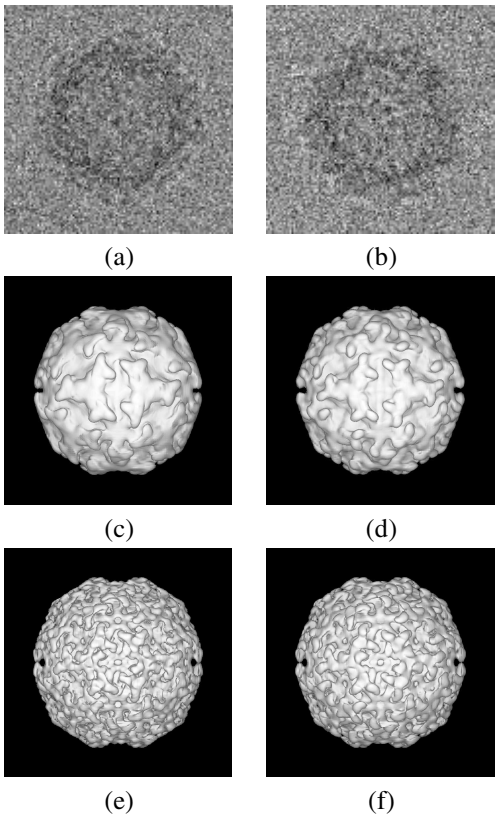

Fig. 1. Reconstructions of the capsid of $N\omega V$. (a,b) Examples of the boxed $N\omega V$ images. Both panels use the same intensity scale. (c,d) Surface plots of the 3-D reconstructions of $N\omega V$ by the previous and the fast algorithms, respectively. (e) The resolution used to compute the synthetic cryo-EM images. (f) The resolution of the recontruction in (c) and (d). The correlation coefficients between (c) and (f) is 0.9429, and between (d) and (f) is 0.9478. The correlation coefficients between (c) and (d) is 0.9945.

which the images are created is known, we can compare the reconstructions with truth. The synthetic data used for the reconstructions are 200 boxed images each measuring 117×117 pixels with a pixel sampling interval of 4.7Å. The projection orientations are uniformly distributed, and the origin offsets of different images are also uniformly distributed over a disk of radius 2 pixels (9.4Å). The SNR of these images, computed by the method in [1, Sec. 2.8], is 0.2. We compute two reconstructions using the previous and the fast algorithms assuming that the origin offsets in the boxed images are zero, which implies that the expectation step requires only 3-D numerical integrals for the unknown orientation. Both previous and the fast algorithm softwares progressively increase the resolution from step 1 to 7 for computational efficiency and because the radius of convergence is larger for lower resolution reconstructions, and each step uses different number of initial conditions [1, Table 1]. Both reconstructions are computed on the 20 clustered dual processor PC nodes. Fig. 1 shows examples of the boxed $N\omega V$ images and two reconstructions from the previous and the fast algorithms. To measure errors, correlation coefficients between each reconstruction and the true structure with the same resolution used to compute the two reconstructions are computed and provided in Fig. 1. Table I shows the average computation time per iteration and the total computation time for both algorithms for step 1–7. The total computation time is huge compared to the average computation time per iteration because precomputing various components in the formulas is so extensive.

TABLE I

COMPUTATION TIME OF THE $N\omega V$ RECONSTRUCTIONS BY THE PREVIOUS AND THE FAST ALGORITHMS.

Step	*computation time / iteration (sec)*		*total computation time (hr:min:sec)*	
	previous	fast	previous	fast
1	0.080	0.020	00:05:56	00:05:59
2	0.603	0.044	00:04:40	00:06:23
3	1.808	0.080	00:09:46	00:17:29
4	4.883	0.157	00:45:51	00:34:47
5	10.839	0.283	02:38:37	01:21:20
6	53.153	1.427	08:52:42	03:21:46
7	212.917	7.130	25:23:01	11:55:08

IV. CONCLUSIONS

A fast algorithm for maximum likelihood 3-D reconstruction from unoriented cryo EM of viruses is described and demonstrated on synthetic boxed images of the capsid of $N\omega V$. The fast algorithm works successfully from the viewpoint of both computation time and the reconstruction. Therefore, especially by exploiting opportunities for speed enhancement, it will be possible to scale up these calculations to address much more challenging problems such as higher resolution 3-D reconstructions of multiple viruses from mixtures of cryo EM images. Results from real data and mixtures of cryo EM images will be reported on in a future publication.

REFERENCES

[1] Z. Yin, Y. Zheng, P. C. Doerschuk, P. Natarajan, and J. E. Johnson, "A statistical approach to computer processing of cryo electron microscope images: Virion classification and 3-D reconstruction," *J. Struct. Biol.*, vol. 144, no. 1/2, pp. 24–50, 2003.

[2] Z. Yin, Y. Zheng, and P. C. Doerschuk, "An *ab initio* algorithm for low-resolution 3-D reconstructions from cryo electron microscopy images," *J. Struct. Biol.*, vol. 133, no. 2/3, pp. 132–142, Feb/Mar 2001.

[3] P. C. Doerschuk and J. E. Johnson, "*Ab initio* reconstruction and experimental design for cryo electron microscopy," *IEEE Trans. Info. Theory*, vol. 46, no. 5, pp. 1714–1729, Aug. 2000.

[4] J. Lee, Y. Zheng, P. C. Doerschuk, J. Tang, and J. E. Johnson, "Maximum likelihood 3-D reconstruction of multiple viruses from mixtures of cryo electron microscope images," in *Proc. of the Electronic Imaging 2005 Symposium*, vol. 5673, San Jose, CA, Jan. 16–20 2005, pp. 336–343.

[5] J. Lee, Y. Zheng, and P. C. Doerschuk, "A fast algorithm for 3-D reconstruction from unoriented projections and cryo electron microscopy of viruses," in *Proc. of the Electronic Imaging 2006 Symposium*, San Jose, CA, Jan. 15–19 2006.

[6] J. Navaza, "On the three-dimensional reconstruction of icosahedral particles," *J. Struct. Biol.*, vol. 144, no. 1/2, pp. 13–23, 2003.

[7] M. E. Rose, *Elementary Theory of Angular Momentum*. New York: John Wiley and Sons, 1957.

[8] J. D. Jackson, *Classical Electrodynamics*, 2nd ed. New York: John Wiley, 1975.

[9] S. Munshi, L. Liljas, J. Cavarelli, W. Bomu, B. McKinney, V. Reddy, and J. E. Johnson, "The 2.8Å structure of a $T = 4$ animal virus and its implications for membrane translocation of RNA," *J. Mol. Bio.*, vol. 261, no. 1, pp. 1–10, 9 August 1996.